

Mechanistic Source Term Modeling for Sodium Fast Reactors

A. J. Clark¹, M. R. Denman¹, D. Grabaskas²

¹Sandia National Laboratories, Albuquerque, NM, United States of America

²Argonne National Laboratory, Lemont, IL, United States of America

Email contact of main author: Andrew.Clark2@sandia.gov

Abstract. This paper describes a sodium fast reactor mechanistic source term analysis for protected loss of flow (PLOF) accident scenario. Pin failure occurs (but not fuel melting) and radionuclides are transported through the sodium coolant and are eventually released into the cover gas. Seal leakage in the top head of the reactor vessel acts as the pathway for radionuclides to escape into containment. The temperature rise in containment is caused by heat transfer through the reactor vessel head; rather than by radioactive decay or thermal inertia carried by aerosol and gaseous products. Greater than 99% of the total cover gas inventory is deposited inside the reactor vessel. The ratio of environmental releases to initial cover gas inventory for aerosols is on average about 2.5E-06 for all accident scenarios and conditions. Noble gas mass is highest inside containment at the end of 500 hours. The ratio of environmental releases to initial cover gas inventory for the noble gases is about 7.31E-02 for krypton and about 5.29E-03 for xenon.

Key Words: sodium fast reactors; mechanistic source term; Contain-LMR

1. Introduction

To evaluate potential impacts to the public and environment from the accidental release of radionuclides, the U.S. Nuclear Regulatory Commission (USNRC) has made source term analysis an important requirement for new reactor license applications. The USNRC hopes are that future advanced reactor license applications will move away from traditional bounding deterministic source term analysis and use a more realistic mechanistic source term (MST) approach [1-3]. The MST approach has advantages for non light water reactors (LWRs), whose design, fuel and coolant do not align with traditional source terms developed for LWRs [1-3].

The most recent sodium fast reactor (SFR) source term characterization appeared in the General Electric Preliminary Safety Information Document (GE PSID) application to the USNRC in 1987 [4]. *FIG. 1* shows how the GE PSID analysis was parceled across three primary severe accident codes. The GE approach involved running SAS4A/SASSYS-1 [5] simulations of accident sequences to determine the extent of core damage in a given sequence. In their analysis [4] oxide fuel release fractions for core damage bins were transferred to Contain-LMR (CLMR) to model radionuclide and sodium behavior in the cover gas and containment regions. Releases from containment were then passed to the MACCS code to evaluate the environmental impact for these binned sequences.

The methodology used for the MST results and CLMR sensitivity analysis described in this paper is similar to the one performed for PRISM (see *FIG. 1*). However, this analysis uses metallic fuel releases from ANL-ART-49 [6,7], rather than oxide fuel as used in the PRISM design.

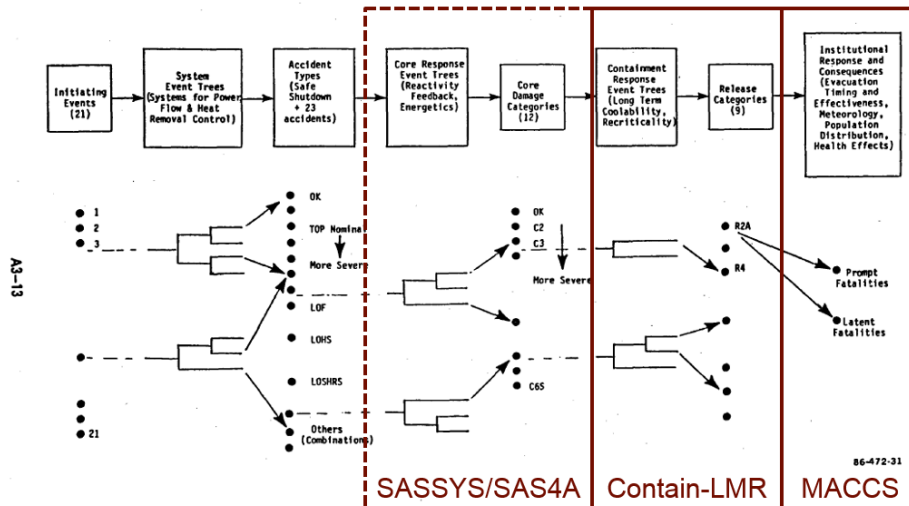


Figure A3.2-1 PRISM RISK MODEL STRUCTURE

FIG. 1. PRISM risk model structure overlaid with dynamic safety codes employed [4].

1.1. Background

Sodium fast reactor (SFR) safety-related gap studies have identified the need for codes supporting MST analyses that can more realistically predict the transportation and retention of radionuclides through the fuel, coolant, and containment [8]. As discussed in ANL-ART-49 [6], initial attempts to utilize the CLMR code [9,10] for the analysis of radionuclide transport encountered code issues, which precluded the use of CLMR results for the trial MST calculation. For example, a code bug would not allow CLMR to model radionuclides as gases. Instead, fission gases would be treated as aerosols which would result in non-conservative estimates of fission gas retention.

An updated version of the CLMR code has addressed the code issues identified in ANL-ART-49 [6]. The MST results and CLMR sensitivity analysis described in this paper use the updated version of the CLMR code and include the following modifications:

- Temperature and pressure responses for the reactor vessel and containment for realistic boundary conditions.
- Fission gases, such as xenon and krypton, are modeled as gases rather than as aerosols. In addition to being able to treat those fission products as gases, their radioactive decay is also modeled in this analysis.
- Sensitivity of aerosol size characteristics are explored here but were not explored in the original analysis.

2. Reference Reactor and Accident Scenarios

In the U.S., SFR vendor reactor designs are typically pool-type designs using metal fuel. Vendor designs have some differences, such as breeder versus burner, sodium coolant temperatures and pressures, and reactor safety systems. For this analysis, the Argonne SFR pool-type design concept from ANL-ART-49 was used. The properties of this reactor important to this analysis are provided in TABLE I.

TABLE I. REFERENCE REACTOR PROPERTIES

| Parameter | Description |
|-------------------------------------|---------------------|
| Reactor Power | 1000 MWth/380 MWe |
| Type | Pool-type |
| Primary Coolant Temp – Inlet/Outlet | 350°/500°C |
| Containment Volume | 8000 m ³ |
| Containment Design Basis Leak Rate | 1.0% Vol/Day |

2.1. Reference Reactor Source Term

ANL-ART-49 [6] predicted the amount of radionuclides that can potentially escape to the cover gas region as a result of two transient scenarios. The reference fuel used for these calculations is based on U-Pu-Zr metal fuel surrounded by a sodium bond with HT-9 cladding material. The reactor consists of 180 fuel assemblies with three core fuel batches and 271 fuel pins per assembly.

2.1.1. Transient Scenarios

ANL-ART-49 used two distinct types of reactor transient scenarios for the MST calculation [6]. One transient scenario is a severe unprotected transient overpower, also referred to as UTOP+. The primary characteristics of the UTOP+¹ scenario are that primary system conditions remain near their nominal conditions, but the core experiences a rapid temperature rise that leads to fueling melting and pin failure. The UTOP+ scenario is associated with a single release of fission products from the fuel.

The other transient scenario is a protected loss of flow (and heat sink) with degraded decay heat removal; this transient is referred to as PLOF+¹. The PLOF+ transient scenario is associated with a slow rise of core temperatures and high primary system temperatures. This transient scenario leads to pin failure due to eutectic penetration with no fuel melting. Near nominal primary system conditions are restored after seven days (168 hours). Three separate releases of radionuclides are predicted, which occur at the following times following the onset of the transient scenario: 22.65 hours, 28.98 hours, and 31.89 hours.

For each transient scenario, four cases were analyzed that vary the amount of radionuclides existing in bubbles and the leakage rate from cover gas to containment. Two bounding estimates for bubble transport of radionuclides from the fuel pin to the cover gas; 10% of the predicted radionuclides or 100% of the predicted radionuclides. And two estimates for leakage rates through the reactor head as a function of the leakage area; 0.0645 cm² and 6.45 cm².

Only one case was used to generate the MST and CLMR sensitivity analysis results described in this paper. ANL-ART-49 predicted that the PLOF+ with 100% radionuclides in bubbles and a leak area of 6.45 cm² led to the largest releases to containment and correspondingly, to offsite release and doses and was used as the source term for the MST and CLMR sensitivity analysis results described in this paper.

3. SFR MST Model

3.1. Contain-LMR Treatment of Released Radionuclides

The detailed analysis of in-pin radionuclide distribution, failed pin radionuclide release, radionuclide bubble transport, and sodium pool radionuclide release are provided in ANL-ART-49 [6]. The predicted radionuclide release into the cover gas region is used as an input into CLMR. Contain-LMR then predicts the transportation and deposition of radionuclide

¹ The plus sign has been added to the transient name to indicate that the transient is more severe than the historical UTOP and PLOF definitions, which do not include degraded decay heat removal.

gases and aerosols from the cover gas region to containment, through containment, and the amount of radionuclides released to the environment.

The CLMR code requires radionuclides to be combined into classes in order to model all radionuclides in a single simulation. The approach of combining radionuclides into classes is adopted from MELCOR [11] which combines radionuclides together based on similar physical and chemical properties. Treatment of all the radionuclides is separated by aerosols and gases. The noble gases, namely isotopes of xenon and krypton, are tracked individually through the CLMR fission product models. Noble gas releases are provided in TABLE II. The rest of the radionuclide classes are defined using eight aerosol classes. Aerosol class compositions and the respective mass associated with each release for the PLOF+ scenario are illustrated in TABLE III.

TABLE II. NOBLE GAS ISOTOPE RELEASES FOR PLOF+ SCENARIO.

| Noble Gas Isotope | Mass in First Release | Mass in Second Release | Mass in Third Release |
|-------------------|-----------------------|------------------------|-----------------------|
| Xenon-133 | 7.07E-02 kg | 6.71E-02 kg | 6.94E-02 kg |
| Xenon-135 | 1.62E-03 kg | 1.06E-03 kg | 1.23E-03 kg |
| Krypton-85 | 1.48E-01 kg | 9.33E-02 kg | 3.90E-02 kg |
| Krypton-85m | 4.48E-06 kg | 1.61E-06 kg | 1.05E-06 kg |

TABLE III. AEROSOL CLASS COMPOSITIONS AND RELEASES FOR PLOF+ SCENARIO.

| CLMR Class | Member Elements Predicted for PLOF+ Scenario | Mass of First Release | Mass of Second Release | Mass of Third Release |
|------------|--|-----------------------|------------------------|-----------------------|
| Cs Class | Cs, Rb | 1.05E+01 kg | 5.01E+00 kg | 7.07E-01 kg |
| Ba Class | Ba, Sr | 1.44E+00 kg | 4.74E-01 kg | 7.11E-02 kg |
| I Class | I, Br | 1.67E-01 kg | 9.17E-02 kg | 3.30E-02 kg |
| Ru Class | Ru, Pd, Rh, Se, Te, Sb | 3.43E-02 kg | 2.19E-02 kg | 1.08E-02 kg |
| Mo Class | Mo, Co, Nb, Tc | 3.70E-02 kg | 2.09E-02 kg | 8.40E-03 kg |
| Ce Class | Ce, Np, Pu, Zr | 6.05E-01 kg | 3.70E-01 kg | 2.83E-01 kg |
| La Class | La, Am, Cm, Eu, Nd, Pm, Pr, Sm, Y | 3.92E-01 kg | 2.69E-01 kg | 1.98E-01 kg |
| U Class | U | 1.12E+00 kg | 1.01E+00 kg | 9.65E-01 kg |

3.2. Contain-LMR Model Nodalization

The CLMR model nodalization is comprised of three primary regions:

1. Region one consists of one spatial cell to model the radionuclide transport within the reactor vessel. Region one includes the sodium pool and the cover gas region where radionuclides originate with each release.
2. Region two consists of five spatial cells that represent the containment. The five cells are free of internal structures and region two includes only wall, floor, and roof structures. Using five cells for a large containment space allows investigation of where in containment aerosols are transported (e.g., the periphery versus the reactor vessel head).
3. Region three consists of one cell that approximates an infinite volume to represent the environment outside containment.

Regions one and two are connected with a unidirectional flow path that represents reactor vessel seal leakage from the cover gas to containment. Regions two and three are connected by

a containment leakage rate that is based on the State-of-the-Art Reactor Consequence Analyses (SOARCA) Surry and Sequoya containment models [12]. The dispersion of radionuclides to the environment and the calculated doses are not determined by CLMR; region three only serves as a radionuclide sink.

4. Results for PLOF+

Temperature and pressure responses for reactor vessel and containment are shown in FIG. 2. The PLOF+ scenario is characterized by a slow heat up that peaks at 1124 K at about 70 hours. After reaching its peak temperature, the pool temperature slowly decreases until it reaches a steady state temperature of 788 K. Contain-LMR uses the initial temperature as a boundary condition and a final shutdown temperature cannot be specified. The reactor vessel peak pressure of about $2.40\text{E}+05$ Pa coincides with the reactor vessel peak temperature. Following the peak pressure, the pressure continues to decrease until the end of the simulation. The reason for this behavior is that the flowpath from cover gas to containment does not close during the entire simulation due to limitations in Contain-LMR's dynamic flowpath controls. By having a constantly open flowpath, gases and aerosols are artificially allowed to continually escape and eventually deplete the cover gas region, thereby creating an unphysical vacuum. By forcing all the cover gas to leave the vessel, a conservative release estimate is expected.

Maximum temperatures for cover gas and containment are 979.6 K at about 70 hours and 344 K at the end of the simulation, respectively. Containment temperature continuously increases because of the heat transfer from the reactor vessel head into containment at the region one and region two interface. The maximum containment pressure is about $1.11\text{E}+05$ Pa.

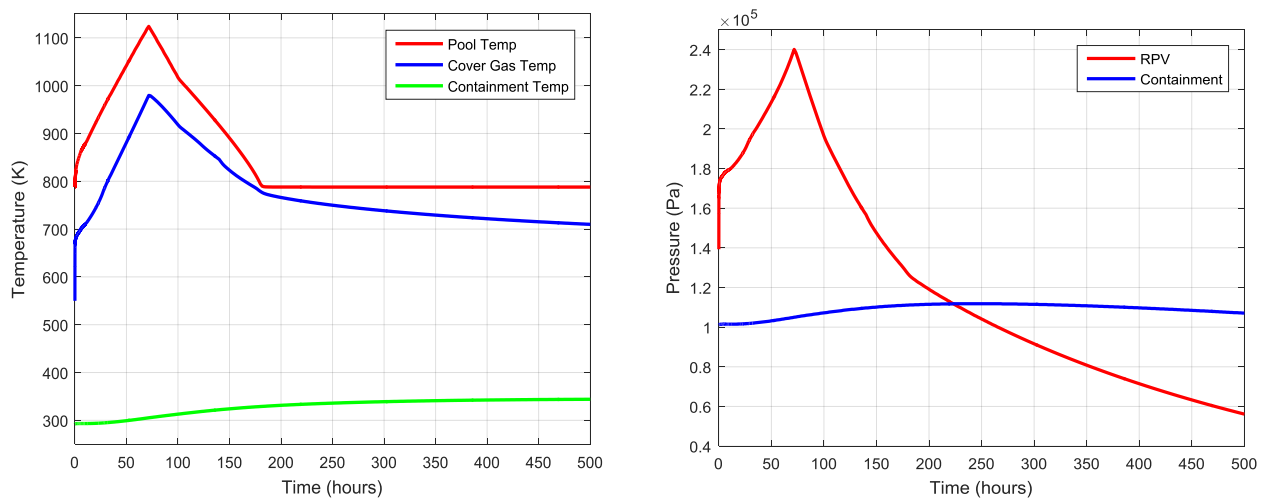


FIG. 2. Reactor vessel and containment temperature (left) and pressure (right) responses through PLOF transient scenario.

FIG. 3 plots the predicted airborne masses of the noble gases in the reactor vessel, containment, and released to the environment. Decrease in the mass of noble gases within the vessel and containment regions as depicted in FIG. 3 are due to transport into the environment and radioactive decay. Krypton-85m and xenon-135 decreases are driven by radioactive decay, with half-lives of 4.48 hours and 9.09 hours, respectively. Krypton-85 is the daughter product of krypton-85m, and increases in mass in both the containment and environment regions. Xenon-133, with a half-life of 5.245 days, has a slow decrease in mass in all three regions due to radioactive decay. For comparison, FIG. 4 shows how xenon-133 is distributed across the three regions.

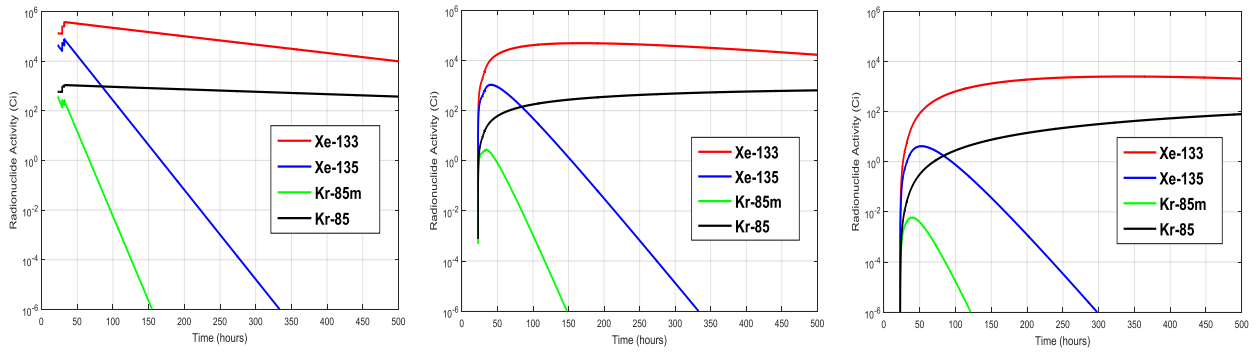


FIG. 3. Noble gas distribution across the three regions: reactor vessel (left), containment (middle), and environment (right).

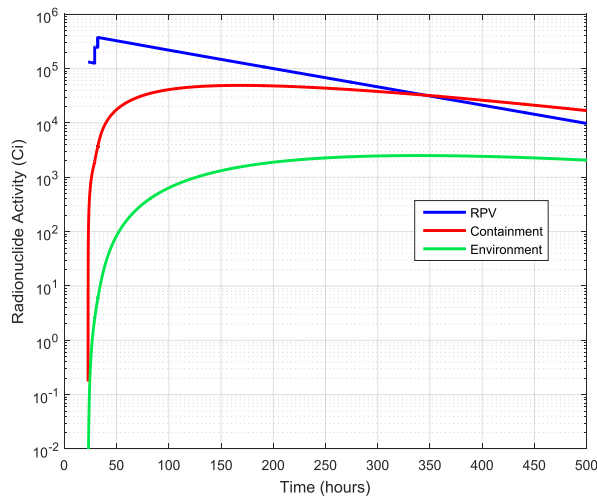


FIG. 4. Xenon-133 gas distribution.

In FIG. 5 the predicted cesium as airborne aerosol and cesium mass deposited is plotted for the three regions. The other aerosol classes follow the same trends seen FIG. 5 in for cesium aerosols. Results show that deposition onto surfaces occurs quickly and that only a fraction of aerosols that originate in cover gas are transported to containment. For the eight aerosol classes, an average of about 0.13% of the aerosol mass is transported from cover gas and into containment. Aerosol deposition in containment is less significant, with an average of about 9.7% of aerosol mass being released from containment.

By the end of the 500 hour simulation, all aerosols have either deposited in the reactor vessel or containment, or have been released to the environment; i.e., no aerosols remain airborne in reactor vessel or containment. Radioactive decay is not modeled for aerosol classes and in this regard, the predicted aerosol masses are a conservative prediction of the source term. The mass of each radionuclide existing in each region at the end of the simulation are shown in FIG. 6.

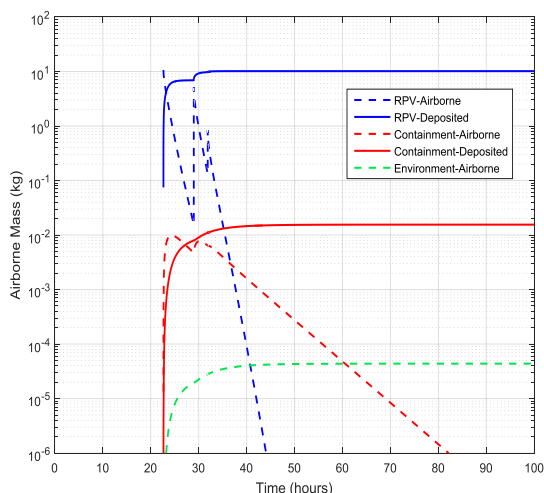


FIG. 5. Cesium aerosol airborne and deposition masses in RPV, containment, and environment.

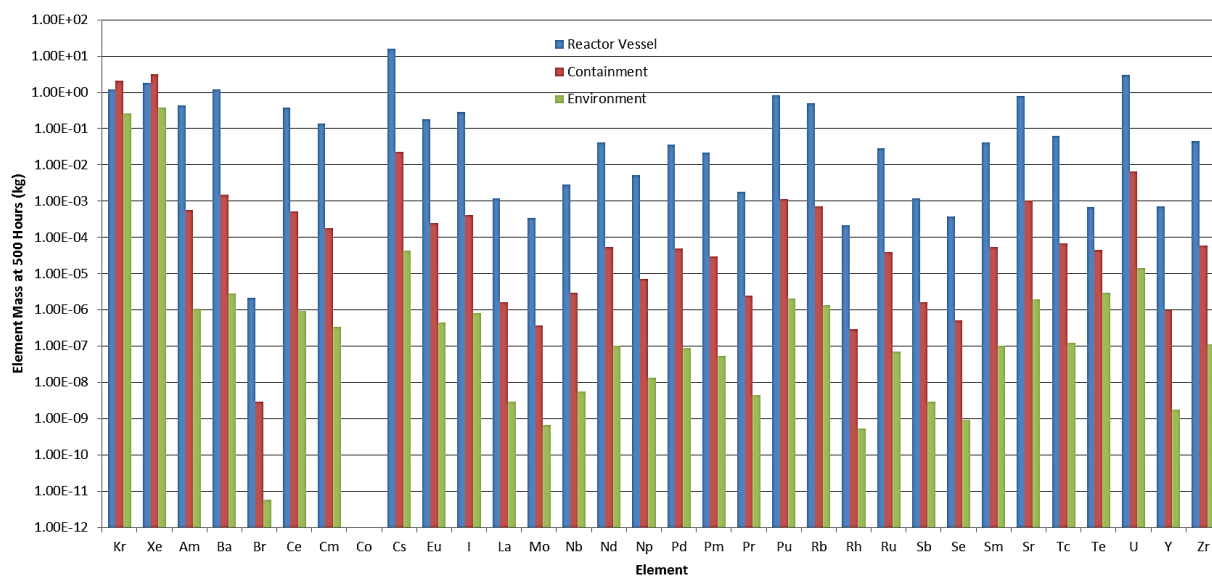


FIG. 6. Elemental distribution across RPV, containment, and environment regions at 500 hours.

5. Aerosol Behavior Sensitivities

Contain-LMR models aerosol transportation and deposition using the MAEROS code [13]. Results are presented from a set of cases that investigate the sensitivity of the CLMR code to selected input parameters that include the surface area to volume ratio, cover gas temperature and aerosol particle size.

5.1. Surface Area to Volume Ratio

The region one volume was reduced to a volume equivalent to include only the cover gas region above the pool. This effectively increased the ratio of surface area to volume from 0.49 to 1.0. The effects of this change are plotted in FIG. 7 for the first release of radionuclides in region one for the PLOF+ case. The deposition rate in MAEROS is directly proportional to the surface area to volume ratio and an increase in the ratio leads to a greater rate of deposition. However, the total amount of deposition inside region one, the reactor vessel, at the end of the simulation is slightly lower when the ratio is 1.0, as a result of a reduction in the effective residence time in region one due to the reduced volume of the region. The mass deposited in region one for this sensitivity case is reduced from 99.86% to 99.80% of the total aerosol mass released.

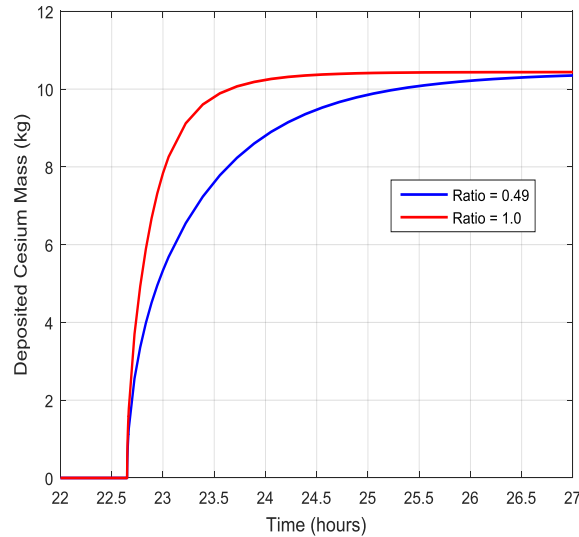


FIG. 7. Deposited cesium mass in reactor vessel following first mass release for surface area to volume ratio sensitivity case.

5.2. Cover Gas Temperature

The atmosphere, in this case the cover gas, temperature also has an effect on the deposition rate. For this sensitivity case, the cover gas was set to 293 K and pool heating was turned off so that the cover gas temperature remained constant for the simulation. FIG. 8 plots the mass of cesium aerosols deposited at 293K and 788K in region one. For CLMR, decreasing the temperature results in decreases in the deposition rate. The total amount of deposition inside the reactor vessel at the end of the simulation is decreased to 99.78% of the total aerosol mass released when the temperature is reduced and pool heating is turned off.

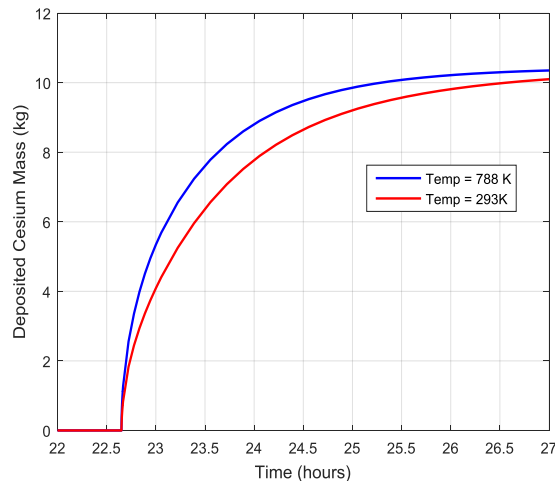


FIG. 8. Deposited cesium mass in reactor vessel following first mass release for cover gas temperature sensitivity case.

5.3. Aerosol Size Sensitivities

FIG. 9 plots the mass of cesium aerosol deposited as a result of changes in the mass median diameter (MMD) and the geometric standard deviation (GSD). The total radionuclide inventory was reduced for this sensitivity case to limit the effects of coagulation and agglomeration of aerosol particles. For the MMD sensitivity, the GSD was set to 1.9 and for the GSD sensitivity, the MMD was set to $7.42E-07 \mu\text{m}$. The total amount of deposition in the reactor vessel at the end of the simulation is only slightly affected by these changes, with the lowest occurring for

MMD equal to $7.42\text{E-}07$ μm and GSD equal to 0.19, where the 99.72% of the total aerosol mass release is deposited inside the reactor vessel.

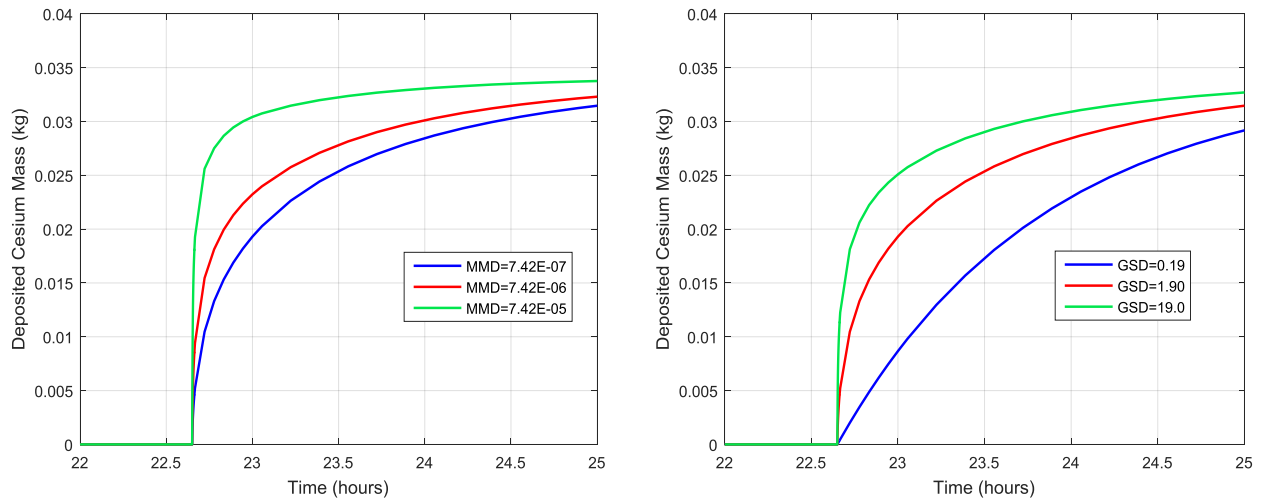


FIG. 9. Deposited cesium mass in reactor vessel following first mass release for MMD (left) and GSD (right) sensitivity cases.

6. Conclusion

An SFR MST analysis can be conducted using the CLMR code to quantify the transportation and deposition of radionuclides throughout the various regions of a nuclear power plant. The CLMR code results presented indicate containment temperatures and pressures will increase slowly. Note, however, that no safety systems are considered in this analysis and therefore the potential effects of safety systems are not included in the estimates of containment response presented in this paper.

Updates to the CMLR code enabled realistic noble gas transport which reduces non-conservative source term estimates calculated in previous CMLR versions. The mass of noble gas released to the environment is several orders of magnitude greater than for the total aerosol mass released. Contain-LMR predicts that about 99.8% of total aerosol mass released into the cover gas is deposited inside the reactor vessel. Sensitivity cases were performed to investigate the parameters affecting deposition.

The sensitivity cases for the selected input parameters demonstrated that although the rate of deposition changes, the total amount of deposition inside the reactor vessel is negligible. The sensitivity case results presented indicate that total radionuclide mass deposited is dominated by the seal leak area and flow rate. Increasing the seal leak area and flow rate allows more aerosol mass to be transported before being deposited, especially for cases where the deposition rate is slow. For large mass releases, coagulation and agglomeration of particles is increased, which leads to larger diameter aerosol particles and consequently, increased deposition. The sensitivity of the CLMR code to coagulation and agglomeration of particles as well as seal leak area and flow rate will be explored in future studies.

References

- [1] U.S. Nuclear Regulatory Commission, “Issues Pertaining to the Advanced Reactor (PRISM, MHTGR, PIUS) and CANDU 3 Designs and their Relationship to Current Regulatory Requirements,” SECY-93-092, 1993.
- [2] U.S. Nuclear Regulatory Commission, “Policy Issues Related to Licensing Non-Light Water Reactor Designs,” SECY-03-0047, 2003.
- [3] U.S. Nuclear Regulatory Commission, “Second Status Paper on the Staff’s Proposed Regulatory Structure for New Plant Licensing and Update on Policy Issues Related to New Plant Licensing,” SECY-05-0006, 2005.
- [4] General Electric Company, “PRISM – Preliminary Safety Information Document Appendix A”, GEFR-00793, 1987.
- [5] T. H. Fanning, “The SAS4A/SASSYS-1 Safety Analysis Code System: User’s Guide,” Argonne National Laboratory ANL/NE-12/4, 2012.
- [6] D. Grabaskas, M. Bucknor, J. Jerden, A.J. Brunett, M. Denman, A. Clark, “Regulatory Technology Development Plan – Sodium Fast Reactor: Mechanistic Source Term – Trial Calculation,” Argonne National Laboratory ANL-ART-49 Vol. 1, 2016.
- [7] D. Grabaskas, M. Bucknor, J. Jerden, “A Mechanistic Source Term Calculation for a Metal Fuel Sodium Fast Reactor,” IAEA Fast Reactor Conference 2017, June, 2017.
- [8] M. Denman, J. LaChance, T. Sofu, G. Flanagan, R. Wigeland, and R. Bari, “Sodium Fast Reactor Safety and Licensing Research Plan – Volume I,” SAND2012-4260, 2012.
- [9] K. K. Murata, D. E. Carroll, K. E. Washington, F. Gelbard, G. D. Valdez, D. C. Williams, *et al.*, “User’s Manual for Contain 1.1: A Computer Code for Severe Nuclear Reactor Accident Containment Analysis,” Sandia National Laboratories, SAND87-2309, 1989.
- [10] K. K. Murata, D. E. Carroll, K. D. Bergeron, and G. D. Valdez, “CONTAIN LMR/1B-Mod. 1, A Computer Code for Containment Analysis of Accidents in Liquid-Metal-Cooled Nuclear Reactors,” Sandia National Laboratories, SAND91-1490, 1993.
- [11] R. Gauntt, R. Cole, C. Erickson, R. Gido, R. Gasser, S. Rodriguez, *et al.*, “MELCOR Computer Code Manual,” NUREG/CR-6119, 2000.
- [12] U. S. Nuclear Regulatory Commission, “MACCS Best Practices as Applied in the State-of-the-Art Reactor Consequence Analyses (SOARCA) Project,” NUREG/CR-7009, 2014.
- [13] F. Gelbard, “MAEROS User Manual,” Sandia National Laboratories, NUREG/CR-1392, SAND80-0822, 1982.